Dilute Polymer Blends: Are the Segmental Dynamics of Isolated Polyisoprene Chains Slaved to the Dynamics of the Host Polymer?

T. R. Lutz, Yiyong He, and M. D. Ediger*

Department of Chemistry, University of Wisconsin−Madison, Wisconsin 53706

Marinos Pitsikalis and Nikos Hadjichristidis

Department of Chemistry, University of Athens, Panepistimiopolis, Zografou 15771 Athens, Greece

Received February 27, 2004; Revised Manuscript Received June 9, 2004

ABSTRACT: ^{13}C NMR has been used to investigate the segmental dynamics of isolated polyisoprene (PI) chains in host matrices of polybutadiene (PB), poly(vinylethylene) (PVE), and polystyrene (PS). In the dilute regime, where intermolecular concentration fluctuations are minimal, the segmental dynamics of isolated PI chains do not become slaved to the segmental dynamics of the host matrix but are significantly biased toward the dynamics of pure PI. Using the framework of the Lodge−McLeish model, it is shown that self-concentration effects can account for the dilute PI segmental dynamics. The value of self-concentration was determined to be 0.41 for PI segmental dynamics in PVE blends, a value which agrees with findings at higher compositions and which is also in reasonable agreement with the Lodge−McLeish prediction (0.45 for PI). In contrast, the observed self-concentration values for dilute PI blends with PS (∼0.20) and PB (∼0.85) do not agree with the model prediction of 0.45. These results indicate the importance of self-concentration in understanding the component dynamics and the rheology of miscible polymer blends.

Introduction

In the past 30 years, polymer scientists have learned a great deal about how individual chains move in homopolymer melts.[1] On the length scale of chemical bonds, segmental dynamics allow many different conformational states of polymer chains to be explored. On slightly longer length scales, large enough that the length of the end-to-end distance of a small section of the chain is nearly Gaussian, Rouse modes are the natural basis for chain dynamics. Finally, on even longer length and time scales, entanglements have a strong influence on chain dynamics, and often the reptation description is employed. Many aspects of the relationship between segmental, Rouse, and terminal relaxation times are understood quantitatively in homopolymer melts.[2,3]

In contrast, our understanding of how individual chains move in a miscible polymer mixture is much more primitive. Consider the question: *How does an isolated chain of polymer A move when completely surrounded by chains of polymer B?* Although this is the simplest possible realization of a polymer blend, only a few papers have even come close to addressing the dynamics of dilute A chains.[4−9] Here we report the segmental dynamics of polyisoprene (PI) chains that are dilute entities in matrices of three other polymers. Our measurements are done with ^{13}C NMR, and we utilize polyisoprene chains that have been enriched in ^{13}C in order to achieve the sensitivity required to address this question.

One possible result of this investigation would be that the isolated A chains are completed trapped by the B chains and not allowed to move on any time scale faster than the time scale of motion of the B chains. Despite the physical appeal of this view, it is absolutely inconsistent with the data presented here. Dilute PI chains in a matrix of either poly(vinylethylene) (PVE) or polystyrene (PS) relax on the segmental length scale much more rapidly (up to a factor of 100 times faster) than the matrix chains that completely surround them. In fact, the segmental relaxation of the dilute PI chains is much closer to the time scale for relaxation in pure PI than it is to the segmental relaxation times of the matrix chains.

These results have important implications for our understanding of dynamics in miscible binary polymer blends. In the composition regime where the mass of the constituent polymers is more nearly balanced, it has often been observed that the two components maintain distinct dynamics, even though the chains are intimately mixed.[4,6,7,10−42] At the blend T_g, the average segmental relaxation times of the two components can differ by 4 or more decades. Differences between the monomer friction coefficients that characterize terminal dynamics can also differ by several decades. For both segmental and terminal relaxation, the dynamics of the two components can also show significantly different temperature dependences.

A variety of models have been used to explain the distinct component dynamics previously reported in miscible polymer blends.[26−28,33,43−46] A physically appealing group of models explains these observations in terms of the average local environment of the two types of polymers; if polymer A is typically found in environments which are richer in A than the overall composition, then the dynamics of polymer A will be biased toward those of pure polymer A. *Intermolecular concentration fluctuation models* postulate that polymers of type A will on average be found in environments biased toward A if the interaction parameter $\chi > 0$. *Self-concentration models* argue that intramolecular connectivity results in A segments always being found in environments which are enriched in A; each segment

* Corresponding author. E-mail: ediger@chem.wisc.edu.

10.1021/ma049605w CCC: $27.50
Published on Web 07/28/2004

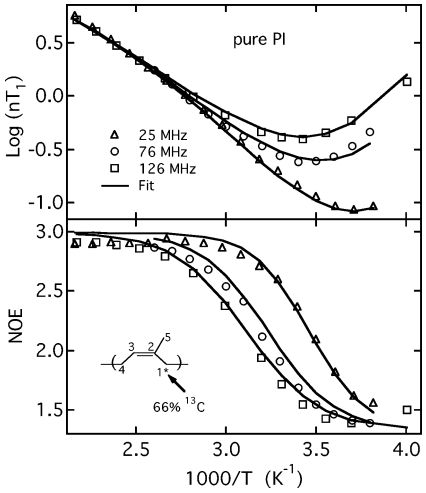

Figure 1. ^{13}C nT_1 and NOE values for the C1 carbon of pure PI obtained at 25, 76, and 126 MHz. Solid lines show the fit obtained by simultaneously fitting all the data to eqs 1−6 with B constrained to 425 K. Fit parameters are shown in Table 2.

Table 1. Characterization of Homopolymers

polymer	M_n (g/mol)	M_w/M_n	T_g (°C)	% PI in blend
polyisoprene (PI)[a]	900	1.39	−83	
1,4-polybutadiene (PB)[b]	2300	1.05	−103	5, 10
poly(vinylethylene) (PVE)[c]	2500	1.04	−33	2
polystyrene (PS2)	1860	1.08	62	2
polystyrene (PS11)	11000	1.05	82	5

[a] 68% *cis*-1,4, 20% *trans*-1,4, 12% 3,4. [b] 90% 1,4-polybutadiene. [c] 89% 1,2-polybutadiene.

in the middle of an A chain is guaranteed to have A segments attached to it on either side.

Our new results show that distinct component dynamics are observed in miscible polymer blends even when one component is completely surrounded by chains of another polymer. Since intermolecular concentration fluctuations are unimportant in the dilute regime, they cannot be responsible for the observed component dynamics. If one ascribes distinct component dynamics to a composition difference in the average local environment for A and B chains, then these new results indicate that self-concentration effects are quite significant.

Experimental Methods

Materials. Polyisoprene (PI) was synthesized with 66% ^{13}C at the C1 position and 33% ^{13}C at C5 (see inset to Figure 1). The PI was prepared via anionic polymerization and characterized by size exclusion chromatography, using methods described elsewhere.[30] The other four polymers were purchased from Polymer Source, Inc. All polymers are described in Table 1.

Blend Preparation. Two-component miscible blends containing polyisoprene and either PB, PVE, PS2, or PS11 were prepared by solvent casting dilute cyclopentane solutions (approximately 500 mg of total polymer in 50 mL of solvent) containing the desired proportions of polymer for the final blend. Cyclopentane was removed under vacuum until ∼7 mL of viscous liquid remained. This solution was transferred to a NMR tube, and the remaining solvent was removed under vacuum. As the viscosity increased with removal of cyclopentane, the solution was coated as a thin film on the wall of the NMR tube and held under vacuum for at least 48 h to ensure complete removal of solvent. The resulting blend was subsequently heated and allowed to flow to the bottom of the NMR tube and sealed under vacuum.

The concentrations of PI in the various dilute blends were chosen to be near or below the overlap volume fraction ($\phi^* = N\nu_0/[(4\pi/3)R_g^3] = 0.05$, where N is the degree of polymerization and ν_0 is the PI monomer volume). PI blends of 2 and 5 wt % were originally prepared with PVE, PS2, and PS11. NMR measurements were sufficiently sensitive to allow measurements on the 2% blends, and these are reported here. For PI/PS11, the 2% blend was inadvertently destroyed; consequently, data from the 5% blend is reported. Because of spectral overlap with PB, higher concentrations of the isotopically labeled PI were required to achieve adequate spectral resolution at low frequencies and low temperatures. Both 5% and 10% PI/PB blends were analyzed at 126 MHz. PI chains were found to have nearly identical T_1 and NOE values in these blends. As a result, we have investigated and present herein only the10% PI/PB blend results.

***T*$_g$ and Miscibility.** Differential scanning calorimetry thermograms were obtained using a Netzsch 200 DSC calibrated to a heating rate of 10 K/min using melting point standards. Samples were hermetically sealed in Netzsch DSC pans. Table 1 includes the homopolymer T_g values.

For polymers with molecular weights similar to those used here, previous work has shown blends of PI with PB,[47,48] PVE,[45,46,49] and PS[50,51] to be miscible over the composition and temperature range relevant for this study.

NMR Measurements. Spin−lattice relaxation (T_1) and nuclear Overhauser enhancement (NOE) measurements were performed using ^{13}C NMR spectroscopy. The T_1 measurements were performed using the standard inversion recovery ($\pi-\tau-\pi/2$) pulse sequence. T_1 is the time required for the magnetization to return to its equilibrium state after an initial inversion. NOE is the ratio of ^{13}C signal intensity when continuous ^{1}H decoupling is employed to the intensity obtained with the use of inverse gated ^{1}H decoupling (decoupling is employed only during acquisition of the ^{13}C spectrum).

^{13}C NMR measurements were performed at three frequencies using two different NMR spectrometers: Varian Inova-500 NMR spectrometer (125.8 MHz) and Bruker DMX-300 (25.1 MHz, 75.6 MHz). On both spectrometers, temperature was controlled to ±0.5 K and calibrated to an uncertainty of ±2 K using an ethylene glycol thermometer, melting point standards, or both. Data were processed with line broadening equal to one-tenth the line width of the spectrum. The magnetization recovery curves for spin−lattice relaxation measurements were fit with three parameters to obtain T_1. Peak intensity and peak area were both used to determine T_1 and NOE and yielded values that agreed to within the experimental error. A minimum of three trials was averaged to obtain the results presented here for T_1 and NOE. The uncertainty in T_1 is ±4% while the uncertainty in NOE ranges from 4 to 6%.

NOE data for the PI/PS blends showed features that we have not previously observed in polymer blends. In acquiring NOE, recovery times between successive scans of 20 times T_1 were required rather than the usual delay of 8−10 times T_1. We tentatively attribute this to magnetization transfer from a ^{13}C spin with a longer T_1. This effect results in a larger uncertainty in NOE for the PI/PS blends (±6%); this phenomenon is not observed in the PI/PVE or PI/PB systems (±4% errors in NOE). The impact of this effect on the reported segmental correlation times for dilute PI in PS is likely to be negligible, as it would not significantly affect the T_1 measurements, which are well described by our fitting procedure.

The temperature range of the measurements was dictated by adequate spectral resolution of the PI C1 peak at low temperatures and generally set to a maximum of 470 K at high temperatures so as to prevent PI degradation. Some samples were taken above 470 K for short periods of time, after which T_1 was reacquired at lower temperatures as a test of sample degradation. In all cases, T_1 measurements after exposure to high temperatures agreed with earlier experiments to within experimental error.

Data Interpretation

NMR Relaxation Equations. Relaxation of the ^{13}C nuclear spin by dipole−dipole coupling is the only significant relaxation mechanism for the sp^3 C1 carbon of PI studied here. Under these conditions, ^{13}C T_1 and NOE are expressed in terms of the spectral density function $J(\omega)$ in the following equations:[30,52,53]

$$\frac{1}{T_1} = Kn[J(\omega_H - \omega_C) + 3J(\omega_C) + 6J(\omega_H + \omega_C)] \quad (1)$$

$$\mathrm{NOE} = 1 + \frac{\gamma_H}{\gamma_C}\left[\frac{6J(\omega_H + \omega_C) - J(\omega_H - \omega_C)}{J(\omega_H - \omega_C) + 3J(\omega_C) + 6J(\omega_H + \omega_C)}\right] \quad (2)$$

In these expressions, $\omega_H/2\pi$ and $\omega_C/2\pi$ are the Larmor frequencies of the ^1H and ^{13}C nuclei, n is the number of protons directly bonded to the carbon of interest ($n = 2$ for C1 of PI), γ_H and γ_C are the gyromagnetic ratios of ^1H and ^{13}C, and K is a constant that depends on the $^1H-^{13}C$ bond length (2.29×10^9 s^{-2}). $J(\omega)$ is the spectral density function and is the Fourier transform of the orientation autocorrelation function $G(t)$ for the C−H bond:

$$J(\omega) = \frac{1}{2}\int_{-\infty}^{\infty} G(t)e^{-i\omega t}\,dt \quad (3)$$

$G(t)$ is the function of our interest because it describes the average reorientation behavior of individual C−H bonds:

$$G(t) = \frac{3}{2}\langle\cos^2\theta(t)\rangle - \frac{1}{2} \quad (4)$$

Here $\theta(t)$ is the angle of the C−H bond relative to its orientation at time $t = 0$. In this paper, we report information about the segmental dynamics of PI obtained from $G(t)$ for C−H vectors on carbon C1 (see inset to Figure 1). Previous work has shown that the reorientation of C−H vectors at carbons C1, C3, and C4 are quite similar to each other.[30]

Correlation Function and Correlation Time. We assume a modified Kohlrausch−Williams−Watts (mKWW) functional form for the orientation autocorrelation function $G(t)$. This functional form has been previously employed and found to give excellent agreement with experimental data and computer simulations:[23,54,55]

$$G(t) = a_{lib}e^{-t/\tau_{lib}} + (1 - a_{lib})e^{-(t/\tau_{seg})^{\beta}} \quad (5)$$

The mKWW function indicates that C−H vector reorientation occurs via two mechanisms: librational and segmental motions. In this equation a_{lib} and τ_{lib} are the amplitude and relaxation time for librational motion; τ_{lib} is set to 1 ps in our fitting analysis as the fit is insensitive to τ_{lib}. The remaining two parameters in this equation, τ_{seg} and β, describe the characteristic segmental relaxation time and the distribution of relaxation times associated with it. We additionally assume that τ_{seg} follows a Vogel−Tammann−Fulcher (VTF) temperature dependence:

$$\log\left(\frac{\tau_{seg}}{\tau_\infty}\right) = \frac{B}{T - T_0} \quad (6)$$

Table 2. Fit Parameters[a] for PI Segmental Dynamics in the Melt and Blends (Eqs 5 and 6)

blend	T_0 (K)	τ_∞ (ps)	a_{lib}	β
pure PI	164	0.33	0.39	0.60 ± 0.10
2% PI/PVE	186	0.43	0.51	0.64 ± 0.15
5,10% PI/PB	155	0.39	0.36	0.54 ± 0.15
2% PI/PS2	254	0.40	0.61	0.55 ± 0.15
5% PI/PS11	256	0.17	0.42	0.38 ± 0.15

[a] B constrained to 425 K.

where τ_∞, B, and T_0 are constants for a given component in a blend. The correlation time for segmental dynamics $\tau_{seg,c}$ is the time integral of the segmental portion of the correlation function:

$$\tau_{seg,c} = \frac{\tau_{seg}}{\beta}\Gamma\left(\frac{1}{\beta}\right) \quad (7)$$

($\tau_{seg,c}$ is also the first moment of the segmental relaxation time distribution.) When discussing segmental dynamics in the following sections, we emphasize $\tau_{seg,c}$ rather than τ_{seg} because the former quantity is determined more robustly in the fitting procedure; i.e., if a number of different sets of fit parameters can adequately describe a data set, the variation in $\tau_{seg,c}$ is generally smaller than the variation in τ_{seg}.

Results

Pure PI. NMR measurements of T_1 and NOE were performed on the C1 carbon of pure PI over a broad temperature range and at three magnetic fields (^{13}C resonance frequencies of 25, 76, and 126 MHz). The results for pure PI as well as the best fit to the data obtained using eqs 1−6 are presented in Figure 1. The fit parameters from eqs 5 and 6 for pure PI are presented in Table 2. For all the fits, B was constrained to 425 K. This constraint was added because T_0 and B are strongly correlated over the investigated range of segmental correlation times. This value of B was chosen as it has been employed in a previous study of PI in PVE,[30] and it also provides an excellent fit to the data. The slight discrepancy between the NOE data and fit at high temperature is likely due to longer length scale relaxation processes not included in eq 5.[55,56]

The fit parameters for pure PI in Table 2 have quantitative significance as the accessible temperature range is broad, and the data go through the T_1 minimum; these factors increase the sensitivity of the fitting procedure. Because of a narrow temperature range and the absence of a T_1 minimum for some of the blends studied, caution should be exercised when making a quantitative interpretation of the blend fit parameters. However, we consider the resulting correlation times ($\tau_{seg,c}$) to be robust in all cases as very similar values were obtained for all successful fits.

The segmental correlation times for pure PI (calculated using the parameters in Table 2 and eq 7) are shown in Figure 2 as the thick solid line. The error in the correlation times for pure PI is 0.25 decade at low temperatures and diminishes to less than 0.1 decade at high temperatures (representative error bars are shown).

2% PI in PVE. NMR measurements for 2% PI in PVE are presented in Figure 3. Fitting the NMR data with eqs 1−6 allows a quantitative evaluation of the effect of blending on segmental dynamics. The fit obtained for 2% PI in PVE is very good (solid lines), and the fit

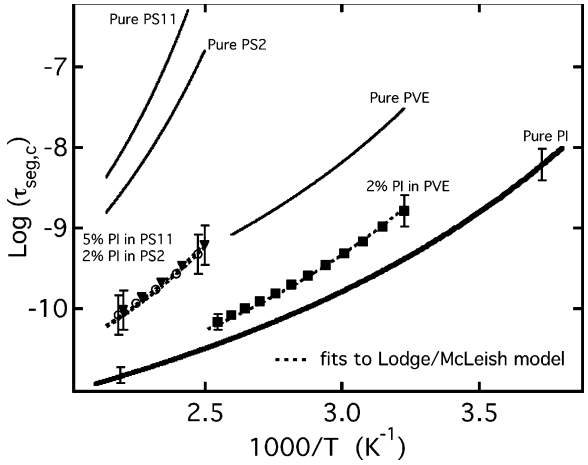

Figure 2. Segmental correlation times for pure PI and the PI component in blends with PVE, PS2, and PS11. Pure PVE, PS2, and PS11 correlation times are given (solid lines as labeled in figure). The dark solid line is the correlation time curve for pure PI; calculated using the fit parameters in Table 2. The symbols are the correlation times for dilute PI in the blends calculated using the fit parameters in Table 2. The dashed lines are fits of the LM model to the blend segmental correlation times. Representative error bars are shown.

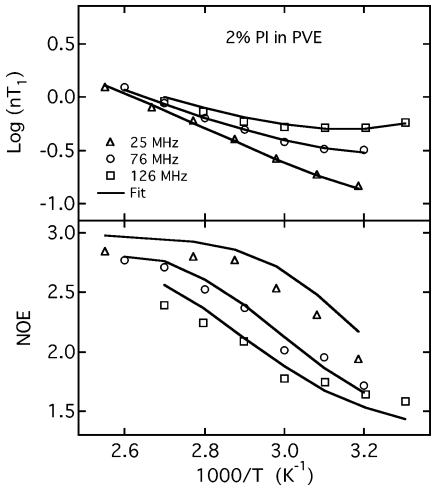

Figure 3. ^{13}C nT_1 and NOE for the C1 carbon of PI in a 2% blend of PI in PVE. Solid lines show the fit obtained by simultaneously fitting all the data to eqs 1−6 with B constrained to 425 K.

parameters are presented in Table 2. The corresponding segmental correlation times for PI in PVE (calculated from fit parameters) are given as filled squares in Figure 2. As expected, since PVE has a higher T_g than PI, PI dynamics in PVE are slowed in comparison to pure PI.

A model independent analysis of the effect of blending on segmental dynamics can be made by directly superposing the blend data onto the pure PI data using temperature shifts. Figure 4 shows that a shift of −26.5 K (not a $1/T$ shift) suffices to superpose the data. The same temperature shift was applied to all frequencies studied and to both the T_1 and NOE data. A small vertical shift was also needed to superpose the T_1 data. From this temperature shift, and the assumption that τ_∞, β, and B are unchanged upon blending, segmental correlation times can be calculated for the isolated PI chains in PVE. These correlation times agree with those shown in Figure 2 to within the error bars indicated. This agreement is an indication of the accuracy of the fitting process described above.

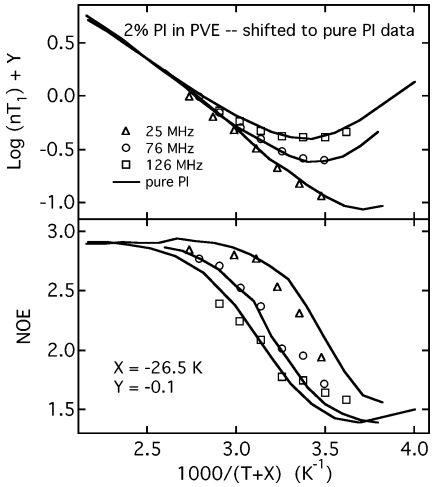

Figure 4. Superposition of 2% PI/PVE blend NMR nT_1 and NOE data points with pure PI data (solid lines). A temperature shift of −26.5 K and a vertical shift of −0.1 were required to get good superposition of the blend data with pure PI data.

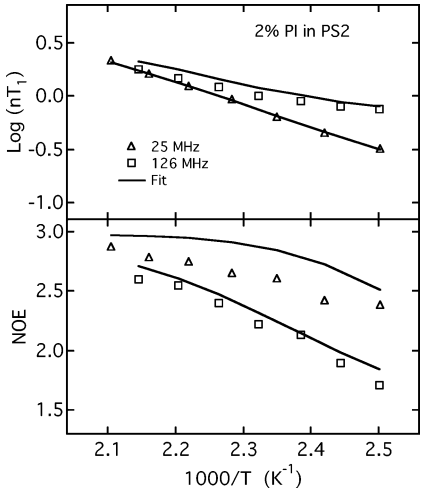

Figure 5. ^{13}C nT_1 and NOE for the C1 carbon of PI in a 2% blend of PI in PS2. Solid lines show the fit obtained by simultaneously fitting all the data to eqs 1−6 with B constrained to 425 K.

2% PI in PS2. NMR results for 2% PI in PS2 are presented in Figure 5 along with fits to the data. The fit quality is fair (fit parameters in Table 2), with some minor discrepancy between the fit and the NOE data. Similar, though slightly smaller, discrepancies occur at high NOE values in Figure 1. The fit parameters yield the segmental correlation times for the dilute PI in PS2 shown in Figure 2 as open circles. Dilute PI dynamics in PS2 are slower than pure PI dynamics, in qualitative agreement with the PI/PVE blend results. The larger influence of PS2 as compared to PVE is consistent with T_g(PS) > T_g(PVE).

The model independent comparison (NMR T_1 and NOE shifts) yields very similar results to those presented in the previous paragraph. Figure 6 shows that a temperature shift of −105 K and vertical shift in log(nT_1) of −0.25 are required to obtain superposition of the data. The rather large vertical shift is expected. Similar superposition shifts were required in a recent study of SISI tetrablocks.[20] Using this temperature shift and τ_∞ and B of pure PI, the segmental correlation times calculated for isolated PI chains in PS2 agree to within

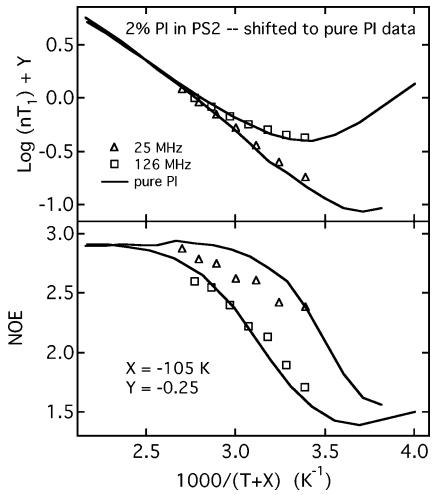

Figure 6. Superposition of 2% PI/PS2 blend NMR nT_1 and NOE data points with pure PI data (solid lines). A shift in temperature of −105 K and a vertical shift of −0.25 are required to achieve the superposition.

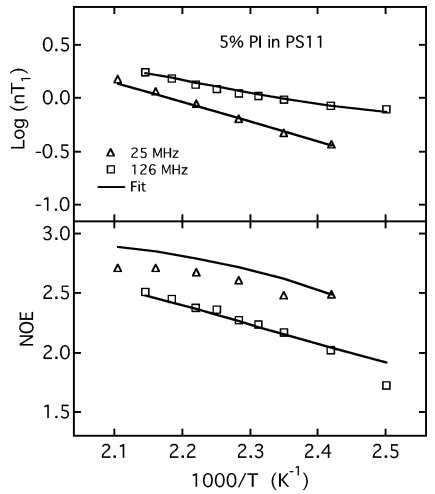

Figure 7. ^{13}C nT_1 and NOE for the C1 carbon of PI in a 5% blend of PI in PS11. Solid lines show the fit obtained by simultaneously fitting all the data to eqs 1−6 with B constrained to 425 K.

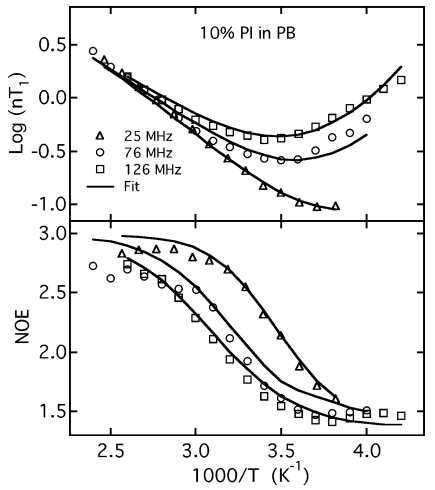

Figure 8. ^{13}C nT_1 and NOE for the C1 carbon of PI in a 10% blend of PI in PB. Solid lines show the fit obtained by simultaneously fitting all the data to eqs 1−6 with B constrained to 425 K.

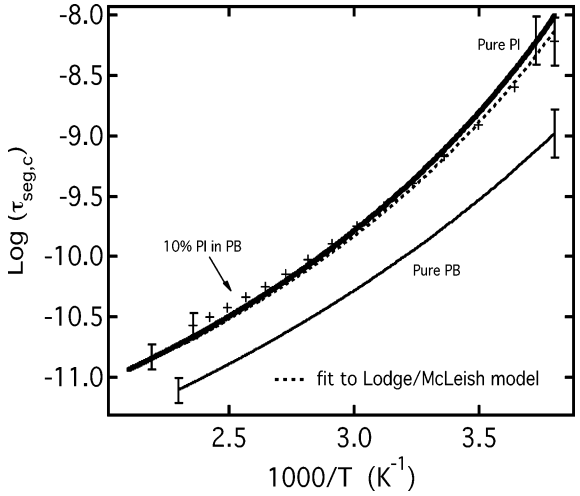

Figure 9. Segmental correlation times for pure PI and PI component in PB. The dark solid line is the correlation time curve for pure PI. It is calculated using the fit parameters in Table 2. The symbols are the correlation times for 10% PI in the PB, also calculated using the fit parameters in Table 2. The dashed line is the fit of the LM model to the blend segmental correlation times. The lower line represents the dynamics of the cis units in pure PB.[67]

the error bars of the correlation times presented in Figure 2.

5% PI in PS11. NMR results for 5% PI in PS11 are presented in Figure 7 along with the fits to the data. The discrepancies between NOE data and the fit are similar to those observed for the 2% PI/PS2 blend; i.e., the fit produces larger NOE values at high temperature than were found experimentally. The segmental correlation times of PI calculated from the fits can be seen as filled triangles in Figure 2. The segmental dynamics of dilute PI in PS11 are similar to the results discussed above for PI in PS2.

The result of NMR data superposition for 5% PI in PS11 (not shown) is nearly identical to the 2% PI/PS2 blend. Applying this temperature shift to T_0 in the VTF equation of pure PI gives segmental correlation times that agree with those presented in Figure 2 for isolated PI dynamics in PS11.

10% PI in PB. NMR results for 10% PI in PB are presented in Figure 8 along with the fits to the data. The fit is very good. The fit parameters are given in Table 2, and the resulting segmental correlation times for PI in PB are shown as crosses in Figure 9. Since the ΔT_g of pure PI and PB is only 20 K, very little temperature shift is expected for dilute PI in PB. In fact, essentially no temperature shift is observed, either from fitting the data to eqs 1−6 (correlation times in Figure 9) or from the model independent superposition of dilute NMR data with that of pure PI (superposition not shown).

Discussion

To what extent does an isolated polyisoprene chain adopt the segmental dynamics of the host chains that surround it? Figures 2 and 9 have the data needed to systematically address this question. In addition to the segmental correlation times of the isolated PI chains and pure PI, segmental correlation times for pure PVE,[30] PS,[23] and PB[57] are also given in these figures.[58] These pure matrix correlation times are a very good approximation to the correlation times of the host chains in mixtures that contain very small amounts of PI. For

our samples of PI in PB, PVE, or PS2, the error associated with this approximation is less than 0.2 decades, while for PI in PS11, the error is at most 0.5 decades.[59]

Figures 2 and 9 clearly show that the segmental dynamics of dilute PI chains in the various blends do not become slaved to the host chain dynamics. In contrast, the dilute chains have dynamics that are substantially different than the host chains and relatively close to the dynamics of pure PI. At a given temperature, we can quantify the extent to which the dynamics of dilute PI chains resemble pure PI dynamics using shifts on the log $\tau_{seg,c}$ scale. In PVE, the dynamics of dilute PI chains shift only 25−30% of the way from pure PI to pure PVE; i.e., dilute PI chains in PVE are 0.4 decades slower than pure PI chains at the same temperature, while the PVE chains in the mixture are 1.5 decades slower than pure PI. In PS, dilute PI dynamics shift about 35% of the way from pure PI to pure PS. A 100% shift on this scale would correspond to isolated PI chains that were completely coupled to the host. A second manifestation of the substantial independence of the dynamics of the dilute PI chains from the host matrix dynamics is found in the temperature dependence. Clearly dilute PI chains in PS do not have the same apparent activation energy as the PS host chains at any given temperature.

Figures 2 and 9 show that the distinct component dynamics that have often been observed in miscible polymer blends persists even into the regime where one polymer is dilute. For blends with component volume fractions near 0.5, distinct component dynamics have sometimes been attributed to intermolecular concentration fluctuations;[26,27,44,50] that is, the segments on a PI chain would retain substantial PI-like dynamics because isoprene segments from other PI chains increase local isoprene concentration. Clearly this explanation cannot be used for the data in Figures 2 and 9. In the limit of isolated chains, intermolecular concentration fluctuations are not present. Thus, if the distinct component dynamics in these dilute systems are to be explained by local concentration arguments, self-concentration effects must be responsible. That is, the segments of a dilute PI chain have PI-like dynamics because other isoprene segments *from the same chain* make the local environment more similar to a pure PI environment than would be expected on the basis of the bulk composition.

It is reasonable to inquire whether the correlation times for dilute PI chains shown in Figure 2 might represent only a subset of all the PI in the mixture; i.e., could there also be a set of much slower PI chains? Evidence for a slow subset would include unusual line shapes and nonexponential magnetization decays. For the 2% PI/PS2 blends, we attempted to model our data with a fast subset with dynamics similar to those shown in Figure 2 and a slow subset comparable to the PS2 matrix dynamics. While the data are consistent with the absence of a slow subset, it would also be consistent with 5% of the PI segments having correlation times as slow as the PS2 matrix.

We next ask whether one particular model based on self-concentration effects, the model of Lodge and McLeish,[28] is consistent with our data.

Lodge−McLeish Model. The Lodge−McLeish (LM) model assumes that the chemical composition of the region within one Kuhn length (l_K) of a given polymer segment determines the mobility of that segment. This local concentration (ϕ_{eff}) is calculated by considering the bulk concentration (ϕ) and the self-concentration (ϕ_{self}):

$$\phi_{eff} = \phi_{self} + (1 - \phi_{self})\phi \tag{8}$$

LM estimate the self-concentration ϕ_{self} as

$$\phi_{self} = \frac{C_\infty M_0}{\kappa \rho N_{av} V} \tag{9}$$

Here C_∞ is the characteristic ratio, M_0 is the repeat unit molar mass, κ is the number of backbone bonds per repeat unit, ρ is the density, N_{av} is Avogadro's number, and $V = l_K^3$.

In this model, polymer segments of a given type have an effective glass transition temperature that is different from the macroscopic blend T_g because ϕ_{eff} differs from ϕ. In our implementation[19] of the LM model, we have used the Fox equation to calculate this effective T_g:

$$\frac{1}{T_g(\phi_{eff})} = \frac{\phi_{eff}}{T_{g,A}} + \frac{1 - \phi_{eff}}{T_{g,B}} \tag{10}$$

We predict segmental dynamics in the blend by correlating changes in $T_{g,eff}$ with changes in T_0

$$T_{0,i}(\phi) = T_{0,i} + [T_{g,i}(\phi) - T_{g,i}] \tag{11}$$

and by assuming that the remaining VTF parameters (B, τ_∞) do not change with blending.

Table 3. Self-Concentration from Data Superposition and from the Lodge−McLeish Fit

	shift		LM fit		LM prediction
blend	ϕ_{self}	range	ϕ_{self}	range	ϕ_{self}
2% PI/PVE	0.40	0.38−0.43	0.41	0.38−0.45	0.45
5,10% PI/PB	1.00	0.70−1.00	0.85	0.60−1.00	0.45
2% PI/PS2	0.16	0.08−0.22	0.22	0.15−0.25	0.45
5% PI/PS11	0.17	0.07−0.27	0.22	0.17−0.27	0.45

Are the Dynamics of Isolated Polyisoprene Chains Consistent with the Lodge−McLeish Model? There have recently been a number of comparisons between experimental data on polymer blends and the LM model near the middle of the composition range.[22,28,44] These comparisons have generally claimed success for the LM model in its ability to fit experimental data, with somewhat less frequent success in its ability to make accurate predictions of ϕ_{self}.[22] In these previous comparisons, disagreements between the model and the data have sometimes been attributed to the presence of intermolecular concentration fluctuations, which are totally neglected in the model. The comparison to dynamics in dilute blends allows for a test of the fundamental assumptions of the LM model in a regime where these concentration fluctuations are irrelevant.

Isolated PI dynamics in the four blends presented in this study can be successfully fit within the framework of the LM model. The dashed lines in Figures 2 and 9 are the LM fits to the dilute PI segmental correlation times using ϕ_{self} as the single fitting parameter; the fitted ϕ_{self} values are given in Table 3. ϕ_{self} values can be obtained either from the temperature shifts needed to superpose the blend data onto the pure PI data (Figures 4 and 6) or from the VTF fitting parameters in Table 2. As shown in Table 3, these two methods yield

consistent ϕ_{self} values. The successful fits shown in Figures 2 and 9 indicate that our data are consistent with the assumption that component dynamics in blends can be described using the pure homopolymer dynamics with a shift in T_0.

We next want to compare the fitted values of ϕ_{self} to the LM prediction. In doing so, we need to consider how the predicted ϕ_{self} for PI (given by eq 9) might change with temperature or environment due to changes in the Kuhn length. Variation in the Kuhn length from a change in temperature is reasonably small for PI in pure PI (<2% over 100 K),[60] and we ignore it here. The effect of environment on the Kuhn length can be estimated from solvent quality studies in dilute solution, from which we expect no change in chain dimensions for these short PI chains.[61] In a direct study, Briber and co-workers show that PS chains of 190 000 g/mol had $\langle r_g^2\rangle^{1/2}$ about 7% larger when dilute in a PVME environment than when in an environment of bulk PS.[62] This result is consistent with the expectation that the environment will have a small effect on the Kuhn length and the predicted ϕ_{self} for low molecular weight chains. Simulations of dilute chains by Sariban and Binder show that changes in chain dimensions can be large but are small for low molecular weight chains in the temperature range of interest.[63]

As discussed above, it is reasonable to consider the predicted ϕ_{self} to be independent of temperature, composition, and blending partner. Under this condition, the LM model (eq 9) predicts a value of ϕ_{self} for PI of 0.45. The results for dilute PI in PVE ($\phi_{self} \approx 0.41$) are consistent with this prediction. In contrast, the fitted values of ϕ_{self} for PI in the two PS blends are roughly 0.2, and the value in the PB blend is roughly 0.8. Given the assumptions made in the derivation of eq 9, factors of order unity may be missing, as pointed out in the LM paper. This comparison would indicate that such missing factors are likely dependent upon blending partner. It is worth noting that the system that shows the largest deviation from the LM prediction for ϕ_{self} (PB) also has the smallest ΔT_g. Because of this, the dynamics obtained from LM using the predicted ϕ_{self} would differ from the measured dynamics by less than 0.5 decades in the temperature range of these measurements.

Is ϕ_{self} Independent of Composition in a Given Blend? In the framework of the LM model, ϕ_{self} does not depend on composition. By comparing our new results to previous studies involving higher PI concentrations, the question of composition dependence can be addressed. ϕ_{self} appears to be composition independent for PI in PI/PVE. The PI/PVE blend has been extensively studied over broad composition and temperature ranges. In a recent paper,[19] it was shown that a self-concentration very close to the LM prediction of 0.45 could accurately reproduce PI dynamics in PVE for PI compositions of 25−75%. This is very close to the ϕ_{self} value found here for dilute PI chains in PVE.

In contrast, for PI/PS blends, ϕ_{self} appears to depend on composition. Because of miscibility issues, blends of PI/PS have not been as extensively studied as the PI/PVE system, so a decisive comparison is more difficult. In recent work on the dynamics in disordered SISI tetrablocks,[21] a ϕ_{self} for isoprene of 0.45 was required to fit the data for volume fractions of 20−77% isoprene. This contrasts with the much smaller ϕ_{self} of ~0.20 obtained for PI in 2% and 5% PI/PS blends. This difference could indicate a composition dependence of the self-concentration for PI in PS. Alternately, concentration fluctuations might be invoked to account for this apparent composition dependence, since $\chi > 0$ in the PI/PS system. It is possible that concentration fluctuations in this system have a substantial impact on the local composition near individual PI segments when the PI concentration is large and that this effect has been lumped into the ϕ_{self} values obtained at these higher concentrations. Because the published data for this system is from disordered tetrablocks and not from blends, additional work would be required to make the above comparison more rigorous.

Comparison to Previous Work. To our knowledge, Adams and Adolf[6] were the first to publish segmental dynamics data on dilute chains in a miscible polymer blend. Their work utilized time-resolved optical spectroscopy of chromophores covalently attached to PI and PVE chains. Their study, which inspired our own work, found that component dynamics were not distinct in the dilute regime. This conclusion is clearly at odds with the results presented here. A number of experimental variables, such as molecular weight, are different in the two studies and potentially explain the different conclusions. At present, we believe it is more likely that the difference arises because the use of chromophores introduces an additional factor, i.e., how the chromophore on chain A couples into the dynamics of the surrounding B chains. Previous work comparing optical and NMR measurements of dilute PI chains in solvents are consistent with the idea that the dynamics of the chromophore are more sensitive to the composition of the environment than is the chain without the chromophore.[64]

Two more recent studies of segmental dynamics indicate distinct component dynamics in the dilute regime. Urakawa used dielectric relaxation to study the segmental dynamics of dilute poly(vinyl methyl ether) (PVME) chains in a PS matrix.[5] He studied concentrations down to 4% PVME, similar to those used here. The PVME segmental relaxation time is in the millisecond range even below the blend T_g, where the PS segmental relaxation times must be at least 10^5 times longer. Lutz et al. used ^{2}H NMR to study the dynamics of dilute d_4-PEO chains in a blend with PMMA, using PEO concentrations as low as 0.5%.[7] In the dilute regime, PEO segmental dynamics are up to 12 orders of magnitude faster than the dynamics of the surrounding PMMA chains. In addition, the PEO segmental dynamics have a much weaker temperature dependence than the PMMA dynamics. Thus, both refs 5 and 7 are clearly consistent with idea that distinct component dynamics can be observed for miscible polymer blends in the dilute regime.

To our knowledge, there are just a few reports of terminal dynamics in a miscible homopolymer blend near the dilute regime. Kim et al.[4] reported diffusion coefficients for both PS and poly(tetramethyl carbonate) (PTMC) in binary blends, including data near or in the dilute regime for each component. They report distinct component dynamics when either the PS or PTMC concentration is small, observing both differing monomeric friction coefficients for the two components and independent temperature dependences for the two monomeric friction coefficients. He et al. recently showed that this PS/PTMC data can be quantitatively fit by the LM model.[22] Watanabe et al.[9] used dielectric relaxation to study to end-to-end vector reorientation of dilute PI

chains in a matrix of PB homopolymers. The temperature dependence of the PI relaxation was consistent with the shift factors for the PB matrix, suggesting the possibility that distinct component dynamics are not observed in this system. In very recent work, Haley and Lodge[8] observed the failure of time−temperature superposition in dilute blends (1%) of PI and PVE in PI/PVE mixtures, thus providing evidence for distinct terminal relaxation dynamics in the dilute regime of this system.

Concluding Remarks

This study probed the segmental dynamics of dilute polyisoprene chains in various host matrices at concentrations near and below the overlap concentration of the polyisoprene. The study was specifically designed to distinguish self-concentration effects from the influence of intermolecular concentration fluctuations. Polyisoprene segmental dynamics were measured at compositions ranging from 2 to 10% in blends with low and high molecular weight polystyrene, poly(vinylethylene), and polybutadiene. Dilute PI chains do not have their segmental dynamics slaved to the host matrix but retain dynamics relatively close to the dynamics of pure PI.

If one takes the view that distinct component dynamics in a miscible blend occur because A and B segments are, on average, in environments with different compositions, our results indicate that the *intramolecular* contribution to these different environments is substantial; i.e., self-concentration effects are very significant. Intermolecular concentration fluctuations may contribute to distinct component dynamics outside the dilute regime. However, for PI in PI/PVE, the simplest view would be that intermolecular concentration fluctuations have no effect on the average component dynamics since PI data at all compositions can be described by the Lodge−McLeish model using a self-concentration that is independent of composition.

The predictions of the Lodge−McLeish model are in quantitative agreement with some of the results presented here, i.e., dilute PI in PI/PVE. In its present form, this model does not accurately predict the segmental dynamics of dilute PI in polystyrene or polybutadiene matrices. If one assumes that the self-concentration expression (eq 9) is correct except that the relevant length scale is not exactly one Kuhn length, then small adjustments of the length scale[65] (values between 0.7 and 1.4 l_K) would suffice to give agreement with all of our experimental data. In this sense, our data strongly support the view of Lodge−McLeish that the relevant length scale for blend dynamics is quite small, at least at the high temperatures probed in this work.[66]

When our dilute data are fit within the Lodge−McLeish framework, the self-concentration values depend significantly upon the blending partner, which suggests that one of the principal assumptions of the Lodge−McLeish approach is not accurate. Although the adjustments in the relevant length scale indicated by these varying self-concentration values are not large, at present we have no means of predicting them. The variations in the self-concentrations values for PI found in this work (0.2−0.8) would produce very significant changes in the predicted blend dynamics for systems with a large T_g contrast. In this sense, additional work is required to develop a model capable of making quantitative predictions of blend dynamics and rheology based only on pure component data.

Acknowledgment. This research was supported by the National Science Foundation through the Division of Material Research, Polymer Program (DMR-0355470). Measurements were performed at the Instrument Center of the Department of Chemistry, University of Wisconsin−Madison, supported by NSF CHE-9508244 and CHE-9629688. Data were analyzed in the computer center in the Department of Chemistry at the University of Wisconsin−Madison, supported by NSF CHE-0091916. We thank Charlie Fry for his support and Paul Nealey for use of his DSC. We also thank the following individuals for their useful comments about this work: Ralph Colby, Jack Douglas, Alan Jones, Sanat Kumar, Tim Lodge, Mike Roland, and Osamu Urakawa.

References and Notes

(1) Doi, M.; Edwards, S. F. *The Theory of Polymer Dynamics*; Clarendon Press: Oxford, 1988.
(2) Adachi, K.; Kotaka, T. *Macromolecules* **1985**, *18*, 466−472.
(3) Smith, G. D.; Paul, W.; Monkenbusch, M.; Willner, L.; Richter, D.; Qiu, X. H.; Ediger, M. D. *Macromolecules* **1999**, *32*, 8857−8865.
(4) Kim, E.; Kramer, E. J.; Osby, J. O. *Macromolecules* **1995**, *28*, 1979−1989.
(5) Urakawa, O.; Sugihara, T.; Adachi, K. *Polym. Appl. (Jpn.)* **2002**, *51*, 10−17.
(6) Adams, S.; Adolf, D. B. *Macromolecules* **1999**, *32*, 3136−3145.
(7) Lutz, T. R.; He, Y. Y.; Ediger, M. D.; Cao, H. H.; Lin, G. X.; Jones, A. A. *Macromolecules* **2003**, *36*, 1724−1730.
(8) Haley, J. C.; Lodge, T. P. *Colloid Polym. Sci.* **2004**, *48*, 463−486.
(9) Watanabe, H.; Urakawa, O.; Yamada, H.; Yao, M. L. *Macromolecules* **1996**, *29*, 755.
(10) Alvarez, F.; Alegria, A.; Colmenero, J. *Macromolecules* **1997**, *30*, 597−604.
(11) Arendt, B. H.; Krishnamoorti, R.; Kannan, R. M.; Seitz, K.; Kornfield, J. A.; Roovers, J. *Macromolecules* **1997**, *30*, 1138−1145.
(12) Arendt, B. H.; Krishnamoorti, R.; Kornfield, J. A.; Smith, S. D. *Macromolecules* **1997**, *30*, 1127−1137.
(13) Chung, G. C.; Kornfield, J. A.; Smith, S. D. *Macromolecules* **1994**, *27*, 5729−5741.
(14) Chung, G. C.; Kornfield, J. A.; Smith, S. D. *Macromolecules* **1994**, *27*, 964−973.
(15) Colby, R. H. *Polymer* **1989**, *30*, 1275−1278.
(16) Doxastakis, M.; Kitsiou, M.; Fytas, G.; Theodorou, D. N.; Hadjichristidis, N.; Meier, G.; Frick, B. *J. Chem. Phys.* **2000**, *112*, 8687−8694.
(17) Fytas, G.; Anastasiadis, S. H.; Karatasos, K.; Hadjichristidis, N. *Phys. Scr.* **1993**, *T49A*, 237−241.
(18) Faller, R. *Macromolecules* **2004**, *37*, 1095−1101.
(19) Haley, J. C.; Lodge, T. P.; He, Y. Y.; Ediger, M. D.; von Meerwall, E. D.; Mijovic, J. *Macromolecules* **2003**, *36*, 6142−6151.
(20) He, Y. Y.; Lutz, T. R.; Ediger, M. D. *Macromolecules* **2003**, *36*, 8040−8048.
(21) He, Y. Y.; Lutz, T. R.; Ediger, M. D.; Lodge, T. P. *Macromolecules* **2003**, *36*, 9170−9175.
(22) He, Y. Y.; Lutz, T. R.; Ediger, M. D. *J. Chem. Phys.* **2003**, *119*, 9956−9965.
(23) He, Y. Y.; Lutz, T. R.; Ediger, M. D.; Ayyagari, C.; Bedrov, D.; Smith, G. K. *Macromolecules* **2004**, *37*, 5032−5039.
(24) Hoffmann, S.; Willner, L.; Richter, D.; Arbe, A.; Colmenero, J.; Farago, B. *Phys. Rev. Lett.* **2000**, *85*, 772−775.
(25) Jack, K. S.; Whittaker, A. K. *Macromolecules* **1997**, *30*, 3560−3568.
(26) Kamath, S.; Colby, R. H.; Kumar, S. K.; Karatasos, K.; Floudas, G.; Fytas, G.; Roovers, J. E. L. *J. Chem. Phys.* **1999**, *111*, 6121−6128.
(27) Kumar, S. K.; Colby, R. H.; Anastasiadis, S. H.; Fytas, G. *J. Chem. Phys.* **1996**, *105*, 3777−3788.
(28) Lodge, T. P.; McLeish, T. C. B. *Macromolecules* **2000**, *33*, 5278−5284.
(29) Milhaupt, J. M.; Lodge, T. P.; Smith, S. D.; Hamersky, M. W. *Macromolecules* **2001**, *34*, 5561−5570.
(30) Min, B. C.; Qiu, X. H.; Ediger, M. D.; Pitsikalis, M.; Hadjichristidis, N. *Macromolecules* **2001**, *34*, 4466−4475.
(31) Ngai, K. L.; Roland, C. M. *Macromolecules* **1995**, *28*, 4033−4035.

(32) Pathak, J. A.; Colby, R. H.; Floudas, G.; Jerome, R. *Macromolecules* **1999**, *32*, 2553−2561.
(33) Roland, C. M.; Ngai, K. L. *Macromolecules* **1991**, *24*, 2261−2265.
(34) Roovers, J.; Toporowski, P. M. *Macromolecules* **1992**, *25*, 1096−1102.
(35) Roovers, J.; Toporowski, P. M. *Macromolecules* **1992**, *25*, 3454−3461.
(36) Salaniwal, S.; Kant, R.; Colby, R. H.; Kumar, S. K. *Macromolecules* **2002**, *35*, 9211−9218.
(37) Schroeder, M. J.; Roland, C. M. *Macromolecules* **1999**, *32*, 2000−2003.
(38) Yang, X. P.; Halasa, A.; Hsu, W. L.; Wang, S. Q. *Macromolecules* **2001**, *34*, 8532−8540.
(39) Zawada, J. A.; Fuller, G. G.; Colby, R. H.; Fetters, L. J.; Roovers, J. *Macromolecules* **1994**, *27*, 6851−6860.
(40) Zawada, J. A.; Fuller, G. G.; Colby, R. H.; Fetters, L. J.; Roovers, J. *Macromolecules* **1994**, *27*, 6861−6870.
(41) Zhang, S. H.; Painter, P. C.; Runt, J. *Macromolecules* **2002**, *35*, 9403−9413.
(42) Zhang, X. Q.; Takegoshi, K.; Hikichi, K. *Macromolecules* **1993**, *26*, 2198−2201.
(43) Kamath, S.; Colby, R. H.; Kumar, S. K. *Macromolecules* **2003**, *36*, 8567−8573.
(44) Leroy, E.; Alegria, A.; Colmenero, J. *Macromolecules* **2003**, *36*, 7280−7288.
(45) Roland, C. M. *Macromolecules* **1987**, *20*, 2557−2563.
(46) Roland, C. M. *J. Polym. Sci., Part B: Polym. Phys.* **1988**, *26*, 839−856.
(47) Jeon, H. S.; Nakatani, A. I.; Han, C. C.; Colby, R. H. *Macromolecules* **2000**, *33*, 9732−9739.
(48) Thudium, R. N.; Han, C. C. *Macromolecules* **1996**, *29*, 2143−2149.
(49) Trask, C. A.; Roland, C. M. *Macromolecules* **1989**, *22*, 256−261.
(50) Rizos, A. K.; Fytas, G.; Semenov, A. N. *J. Chem. Phys.* **1995**, *102*, 6931−6940.
(51) Se, K.; Takayanagi, O.; Adachi, K. *Macromolecules* **1997**, *30*, 4877−4881.
(52) Gisser, D.; Glowinkowski, S.; Ediger, M. D. *Macromolecules* **1991**, *24*, 4270−4277.
(53) Doddress, D.; Glushko, V.; Allerhand, A. J. *J. Chem. Phys.* **1972**, *56*, 3683.
(54) Moe, N. E.; Qiu, X. H.; Ediger, M. D. *Macromolecules* **2000**, *33*, 2145−2152.
(55) Qiu, X. H.; Moe, N. E.; Ediger, M. D.; Fetters, L. J. *J. Chem. Phys.* **2000**, *113*, 2918−2926.
(56) Qiu, X. H.; Ediger, M. D. *Macromolecules* **2000**, *33*, 490−498.
(57) He, Y. Y.; Lutz, T. R.; Ediger, M. D., to be published.
(58) Small differences in T_g due to molecular weight differences were accounted for by assuming identical dynamics at constant $T - T_g$.
(59) These errors are estimated by assuming that the matrix segmental correlation times shift with the measured blend T_g values.
(60) Brandrup, J.; Immergut, E. H.; Grulke, E. A. *Polymer Handbook*, 4th ed.; Wiley: New York, 1999.
(61) Tsunashima, Y.; Hirata, M.; Nemoto, N.; Kurata, M. *Macromolecules* **1988**, *21*, 1107−1117.
(62) Briber, R. M.; Bauer, B. J.; Hammouda, B. *J. Chem. Phys.* **1994**, *101*, 2592−2599.
(63) Sariban, A.; Binder, K. *Makromol. Chem.* **1988**, *189*, 2357−2365.
(64) Adolf, D. B.; Ediger, M. D.; Kitano, T.; Ito, K. *Macromolecules* **1992**, *25*, 867.
(65) Kant, R.; Kumar, S. K.; Colby, R. H. *Macromolecules* **2003**, *36*, 10087.
(66) Reference 65 shows that the relevant length scale can grow somewhat as the temperature is lowered towards the blend T_g.
(67) PB correlation times are estimated from NMR data in ref 57 on pure PB. The pure PB had a measured T_g 8 K greater than the PB used in this study. Consequently, a shift of 8 K was applied to the measured PB correlation times to produce the pure PB curve in Figure 9. NMR measurements on the PB sample used here confirmed the expected 8 K shift.

MA049605W